Biomaterials 33 (2012) 3334–3343

Contents lists available at SciVerse ScienceDirect

Biomaterials

journal homepage: www.elsevier.com/locate/biomaterials

Translocation mechanisms of chemically functionalised carbon nanotubes across plasma membranes

Lara Lacerda [a,1,3], Julie Russier [b,3], Giorgia Pastorin [b,2], M. Antonia Herrero [c], Enrica Venturelli [b], Hélène Dumortier [b], Khuloud T. Al-Jamal [a,e], Maurizio Prato [d], Kostas Kostarelos [a,*], Alberto Bianco [b,*]

[a] Nanomedicine Laboratory, Centre for Drug Delivery Research, The School of Pharmacy, University of London, 29-39 Brunswick Square, London WC1N 1AX, UK
[b] CNRS, Institut de Biologie Moléculaire et Cellulaire, Laboratoire d'Immunologie et Chimie Thérapeutiques, 67000 Strasbourg, France
[c] Departamento de Química Orgánica, Facultad de Química, Universidad de Castilla-La Mancha, 13071 Ciudad Real, Spain
[d] Dipartimento di Scienze Farmaceutiche, Università di Trieste, Piazzale Europa 1, 34127 Trieste, Italy
[e] Institute of Pharmaceutical Science, King's College London, Franklin-Wilkins Building, London SE1 9NH, UK

ARTICLE INFO

Article history:
Received 7 November 2011
Accepted 9 January 2012
Available online 30 January 2012

Keywords:
Nanomaterials
Carbon nanotubes
Cell uptake
Inhibitors
Phagocytosis
Endocytosis

ABSTRACT

Understanding the mechanisms responsible for carbon nanotube (CNT) internalisation into live cells is considered critical both from a fundamental point of view and for further engineering of CNT-based delivery systems to intracellular targets. While several studies are focused on the development of such CNT-based delivery systems, attempts to systematically elucidate the cellular uptake mechanisms of CNTs are still rather limited. The aim of the present study is to evaluate the cellular internalisation of chemically functionalised multi-walled carbon nanotubes (*f*-MWCNTs) in the presence of different well-known cellular uptake inhibitors. Our data reveal how *f*-MWCNTs are able to translocate across cell membranes of both phagocytic and non-phagocytic cell lines. We have evidenced that at least 30–50% of *f*-MWCNTs are taken up by cells through an energy-independent mechanism. This characteristic makes nanotubes loaded with therapeutic or diagnostic cargos extremely interesting as the release of active molecules directly into the cytoplasm increase their biological activity and therapeutic efficacy.

1. Introduction

Functionalised carbon nanotubes (*f*-CNTs) are considered promising new materials for the delivery of therapeutic and diagnostic molecules [1–3]. The capacity of *f*-CNTs to readily pass the plasma membrane and enter into the cytoplasm renders them very interesting candidates for the transport of cargos such as proteins, nucleic acids or small drugs [4]. On the other hand, the mechanism of cellular uptake of these nanomaterials remains an issue of debate although two main pathways have been evidenced [5–12]. In fact, it has been demonstrated that *f*-CNTs are able to enter the cells both via an energy-dependent, endosomally-mediated internalisation mechanism and via direct translocation through the plasma membrane into the cytoplasm which has been termed by some as the "nanoneedle" mechanism [13–17].

Between the two possible pathways of internalisation, the nature of the functional groups covalently linked or non-covalently complexed to the CNTs seems to be of great importance. Indeed, the presence of biomacromolecules such as proteins, antibodies or DNA on the nanotube surface has been associated with energy-dependent endocytotic uptake [14,18,19]. It is likely that macromolecules on the tube surface impede direct CNT–cell membrane interactions, rendering the tubes unable to directly cross the plasma membrane. In this context, the interaction of the coating molecules with extracellular receptors that recognise them as ligands could trigger the active process of internalisation of the entire macromolecule-coated CNT complex. This explanation is also coherent with our observations of direct membrane translocation of CNTs chemically functionalised with low-molecular weight molecules through the cellular membrane [8,13]. This passive mechanism allows the direct localisation of *f*-CNTs into the cytoplasm and potentially renders the transported therapeutic agents immediately available to intracellular targets. The role of nanotube dimensions as they interact with cells on the internalisation mechanism has also been confirmed in a recent study where it was

* Corresponding authors.
E-mail addresses: kostas.kostarelos@pharmacy.ac.uk (K. Kostarelos), a.bianco@ibmc-cnrs.unistra.fr (A. Bianco).
[1] Present address: Radiation Oncology Department, MD Anderson Cancer Center, 1515 Holcombe Bldv., Houston, TX 77030, USA.
[2] Present address: National University of Singapore, Department of Pharmacy, 3 Science Drive 2, Block S15, Singapore 117543, Singapore.
[3] These authors contributed equally to this work.

0142-9612/$ – see front matter © 2012 Elsevier Ltd. All rights reserved.
doi:10.1016/j.biomaterials.2012.01.024

demonstrated that carboxylated or amidated CNTs penetrate non-phagocytic cells by direct translocation when well-individualised or via energy-dependent endocytosis when present as small bundles [11]. In another study, cells exhibited different uptake pathways for CNTs with different dimensions in terms of diameter and length [9]. Again, the contribution of both energy-dependent and independent mechanisms was demonstrated and it seems that nanotube length, degree of aggregation (and aggregate dimensions) and surface coat could be critical parameters that can switch uptake mechanisms from one to another [9].

Moreover, it is important to note that the studied cell types will also play an important role in the prevalence of one uptake pathway over another during the internalisation process. Indeed, phagocytic and non-phagocytic cells may exhibit different uptake behaviour due to their difference in biological function. To better elucidate the possible pathways that account for CNT cellular uptake, we here evaluated the internalisation of fluorescently-labelled-MWCNTs in both phagocytic RAW 264.7 murine macrophages and non-phagocytic A459 human lung carcinoma cells in the presence of different well-known active uptake inhibitors by flow cytometry. We further investigated the intracellular presence and localisation of MWCNTs in RAW 264.7 and A549 by confocal laser scanning microscopy (CLSM) and transmission electron microscopy (TEM), respectively.

2. Materials and methods

2.1. MWCNTs

Pristine MWCNTs were purchased from Nanostructured and Amorphous Materials Inc. (USA, Lot No. 1240XH) were 94% pure, with outer diameters between 20 and 30 nm, and lengths between 0.5 and2 μm. MWCNT-NH_3^+ **1** and **2** (Fig. 1) were prepared as described in details elsewhere [20–22]. Fluorescent-labelling of MWCNTs with fluorescein isocyanate (FITC; MWCNT-FITC **3** and **4**) was accomplished by reacting MWCNT-NH_3^+ with FITC in DMF and diisopropylethylamine [21,22].

2.2. Cell culture

Murine RAW 264.7 macrophages were cultured in RPMI 1640 medium supplemented with 10% heat inactivated fetal bovine serum (FBS), 10 μg/ml gentamycin, 50 μM 2-β-mercaptoethanol, 10 mM HEPES, and maintained in controlled atmosphere (37 °C, 5% CO_2). When reached confluency of 70–80%, cells were detached with 2 mM EDTA, and subcultured in 75 cm^2 flasks. Before performing inhibition tests, cells were reseeded in 24 well plates (250,000 cells/well; 400 μl/well) and allowed to adhere 24 h prior to the experimentation. Human lung carcinoma (A549) cells were cultured in F12K media supplemented with 10% FBS and 1% penicillin/streptomycin at 37 °C, 5% CO_2. All the media used for RAW 264.7 culture were obtained from Lonza. A549 cells were maintained and passaged in DMEM media

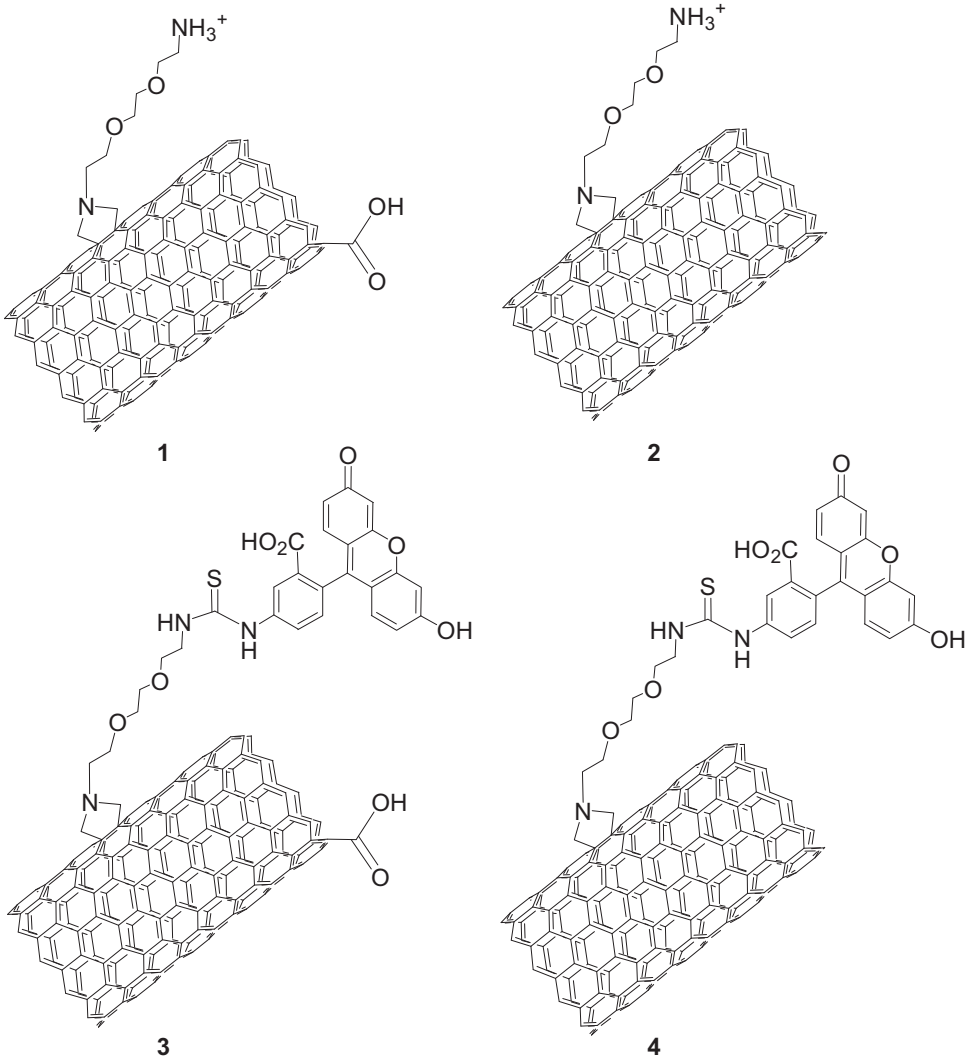

Fig. 1. Molecular structures of functionalised MWCNTs used in this study. The MWCNTs were first made water dispersible through 1,3-dipolar cycloaddition reaction (structure **1** and **2**) and then derivatised with a fluorescent probe, FITC (structure **3** and **4**).

supplemented with 10% FBS, 50 U/ml penicillin, 50 μg/ml streptomycin, 1% L-glutamine and 1% non-essential amino acids, at 37 °C in 5% CO_2. All the media used for A549 culture were obtained from Invitrogen.

For flow cytometry analysis, cells were seeded in 24 well plates 24 h before incubation with the *f*-MWCNTs while they were seeded in transwell inserts (Coostar) 3 days prior the experiment for TEM imaging.

2.3. *f*-MWCNT uptake studies

Internalisation studies included (i) RAW 264.7 and A549 control cells and (ii) RAW 264.7 and A549 cells pre-treated with cellular uptake inhibitors for 30 min and then incubated with MWCNT-FITC **3** or **4** (50 μg/ml and 100 μg/ml respectively) for 120 min or 60 min at 37 °C, respectively. All experiments were conducted in serum-free media. The inhibitors concentrations were preliminarily tested for cytotoxicity and working concentrations were chosen when cellular viability was higher than 70%. All chemicals were obtained from Sigma. Cells were then pre-treated under specific conditions to inhibit different cellular internalisation pathways. The impact of temperature on the cellular internalisation of MWCNT-FITC was studied by pre-incubating RAW 264.7 or A549 cells at 4 °C for 30 min prior to incubation with MWCNT-FITC **3** or **4** at 4 °C for 120 min or 60 min, respectively, while energy-depletion conditions were obtained using NaN_3 (5 mM or 25 mM) in culture medium supplemented with 50 mM of 2-deoxy-D-glucose. To inhibit clathrin-dependent endocytosis, cells were pre-treated with 2 μg/ml or 10 μg/ml chlorpromazine or K^+-depleted with a series of washes following an incubation (30 min at 37 °C) with K^+-free buffer (140 mM NaCl, 20 mM Hepes, 1 mM $CaCl_2$, 1 mM $MgCl_2$, 1 mg/ml D-glucose, pH 7.4). Caveolae-dependent endocytosis was disrupted by pre-treating the cells with 20 μM or 200 μM genistein (2 h at 37 °C) or 0.1 μg/ml or 1 μg/ml filipin. Macropinocytosis was inhibited with 40 μM or 400 μM amiloride or 5 mM methyl-β-cyclodextrin (m-βCD). The inhibitory effects in each internalisation pathway were verified by monitoring the internalisation of fluorescent well-known cellular uptake markers by flow cytometry: transferrin (30 μg/ml) was used as positive uptake marker in 4 °C, NaN_3, K^+-depletion and chlorpromazine (clathrin-mediated endocytosis inhibitor) experiments, Bodipy-LacCer/BSA (0.5 μM) was used as a positive uptake marker in genistein and filipin III inhibitory conditions (caveolae-mediated endocytosis inhibition) and dextran (250 μg/ml) was used as a positive uptake marker in macropinocytosis inhibition tests. These markers were purchased from Molecular Probes. After incubation, cells were washed twice with PBS (RAW 264.7 and A549), detached with 2 mM EDTA (RAW 264.7) or by trypsinisation (A549), stained for fluorescence microscopy (RAW 264.7) or analysed by flow cytometry (RAW 264.7 and A549).

2.4. Flow cytometry analysis

After incubation, cells were washed twice with ice cold PBS in order to remove the excess and unbound MWCNT-FITC, transferrin, Bodipy or dextran from the extracellular media. MWCNT-FITC present at the cell surface were washed out with ice cold 0.04% trypan blue in PBS, pH was adjusted to 3.5 with HCl. The excess of transferrin and dextran at the cell surface was removed with ice cold culture media (pH 3.5) while the excess of Bodipy was washed out with ice cold 5% defatted BSA in PBS (3 × 5 min). Dead cells were excluded from the analysis by addition of the red fluorescent exclusion dye 7-amino-actinomycin D (7AAD) to each sample tested. To quantify the effect of each internalisation mechanism-inhibitory treatment, the mean fluorescence intensity of the tested cells distributions was normalised to the mean fluorescence intensity of the control cells distribution at 37 °C. All conditions were run in triplicate. The mean fluorescence intensity of 20,000 individual cells was measured using a FACS Calibur (BD Biosciences) and analysed using FlowJo software.

2.5. Immunofluorescence

After treatment, RAW 264.7 macrophages were stained for fluorescence microscopy studies. Briefly, cells were detached using 2 mM EDTA, washed twice with TBS and incubated with anti-mouse CD11b-biotinylated primary antibody (BD Pharmingen; 1:100, 1 h at 4 °C). Cells were then washed and incubated with Streptavidin-Alexa^{546} (Molecular Probes; 1:500; 30 min at 4 °C). Cells were then fixed with 4% paraformaldehyde (1 h at 4 °C), nuclei were counterstained with DAPI (Sigma; 0.1 μg/ml, 10 min at room temperature) and cells were finally mounted on glass slides with Vectashield (Vector Laboratories). Images were acquired with a Zeiss Axiovert LSM500 confocal with a 63× oil immersion objective (Carl Zeiss Inc.) applying identical acquisition parameters to all samples.

2.6. Transmission electron microscopy

In order to investigate the cellular internalisation mechanism of *f*-MWCNTs by transmission electron microscopy, A549 cells were washed with PBS and then incubated with MWCNT-NH_3^+ **2** (50 μg/ml) at 37 °C for 15, 30, 60 and 120 min in serum-free media. To study the effect of the temperature on the cellular uptake of *f*-MWCNTs, cells were rinsed with PBS, pre-incubated at 4 °C for 30 min in serum-free media and incubated with MWCNT-NH_3^+ **2** (100 μg/ml) at 4 °C for 30 and 60 min in serum-free media. Cells cultured on filter inserts and treated with MWCNT-NH_3^+ **2** were then washed with PBS and fixed with 3% glutaraldehyde in 0.1 M cacodylate buffer (pH 7.4) at 4 °C overnight. On the following day, after washing the cells 3 times with distilled water, a secondary fixation was carried out with 1% aqueous osmium tetroxide for 60 min. The cells were then rinsed with water and dehydrated in a series of ethanol (70%, 90% and 100%). Infiltration with araldite resin was done using a 1:1 mixture of absolute ethanol and araldite resin mix and neat resin (overnight). The wells were filled with fresh resin and placed into the oven to polymerise the resin at 60 °C for 48 h. Ultra-thin sections (65–85 nm thick) were stained with uranyl acetate and lead citrate, and imaged with a Philips CM10 TEM at 80 kV. Images were captured with a high resolution digital camera.

2.7. Statistical analysis

The experiments shown are a summary of the data from at least three separate experiments run in triplicate. All data are presented ±SEM (standard error of the mean). Statistical analyses were performed using GraphPad software. Treatment effects were analysed using one-way ANOVA, followed by Dunnett's post test. The results $p < 0.05$ were used to indicate the significance.

3. Results

We demonstrated earlier that the cellular uptake of water dispersible, 1,3-dipolar cycloaddition functionalised CNTs (single- and multi-walled) was independent on the chemical moieties present at their surface, or the cell type (prokaryotic and eukaryotic cells) [13]. To further investigate the process by which *f*-MWCNTs enter mammalian cells, cellular internalisation pathways in CNT uptake were assessed by flow cytometry, confocal laser scanning microscopy and TEM imaging in the presence of active cellular uptake inhibitors.

For this purpose, we prepared water-dispersible MWCNTs through the 1,3-dipolar cycloaddition reaction, by which ammonium groups were introduced covalently at the surface of the nanotubes [20–22] (Fig. 1, structures **1** and **2**). These CNTs were then derivatised with a fluorescent probe (FITC; Fig. 1, structures **3** and **4**) and the intracellular uptake of the resultant MWCNT-FITC by RAW 264.7 macrophages and non-phagocytic A549 cells under several conditions (energy depletion, inhibition of clathrin- and caveolae-mediated endocytosis or macropinocytosis, see Table 1) was evaluated by flow cytometry. Control tests were also run using specific and well-known markers for each internalisation pathway. In particular, fluorescently-labelled transferrin was used as an uptake marker for clathrin-dependent endocytosis, LacCer-Bodipy was used as an uptake marker for caveolae-dependent endocytosis and dextran was the uptake marker for macropinocytosis [23,24]. After initial pre-treatment for 30 min with the different inhibitors, RAW 264.7 were exposed to MWCNT-FITC **3** for 2 h (50 μg/ml) while A549 cells were incubated with MWCNT-FITC **4** for 1 h (100 μg/ml). These concentrations and times were initially determined to obtain a good fluorescence signal, distinct from the naïve unstained cell populations (Fig. 2).

Flow cytometry analyses showed that incubating RAW 264.7 or A549 at 4 °C or under energy-depleted conditions (NaN_3) resulted

Table 1
Effect of inhibitors on each internalisation pathway.

Inhibitor	Clathrin-mediated endocytosis	Caveolae-mediated endocytosis	Macropinocytosis
Low temperature (4 °C)	✓	✓	✓
Energy depletion (NaN_3)	✓	✓	✓
K^+-depletion	✓		
Chlorpromazine	✓		
Genistein		✓	
Filipin III		✓	
Amiloride			✓
m-βCD		✓	✓

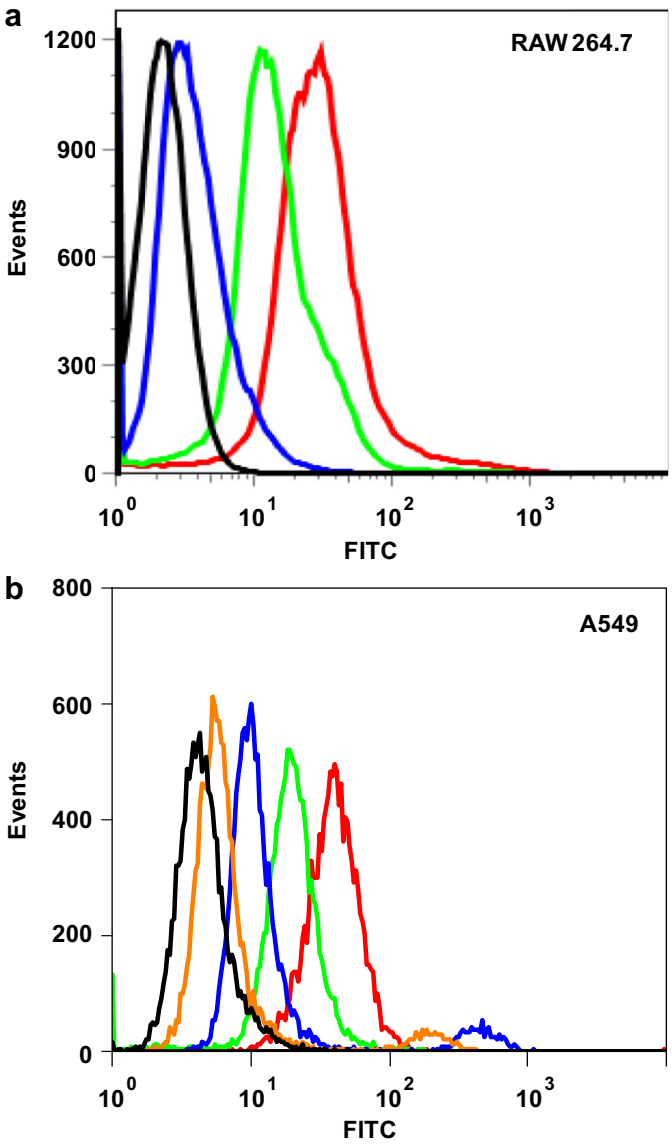

Fig. 2. Quantification of the extent of cellular uptake of MWCNT-FITC **3** and **4** in RAW 264.7 (a) and A549 (b) by flow cytometry. RAW 264.7 macrophages were incubated for 2 h at 37 °C without (black line) and with 2 (blue line), 20 (green line) or 50 μg/ml (red line) of MWCNT-FITC **3**. A549 cells were incubated for 60 min at 37 °C without (black line) and with 5 (orange line), 25 (blue line), 50 (green line) or 100 μg/ml (red line) of MWCNT-FITC **4**. (For interpretation of the references to colour in this figure legend, the reader is referred to the web version of this article.)

in uptake of 30–50% of the nanotubes (Fig. 3a and b). In order to inhibit clathrin-mediated endocytosis, the cells were pre-treated with K^+-depletion medium or chlorpromazine [23,25]. Despite of the pre-incubation with K^+-depletion buffer (RAW 264.7) or chlorpromazine (A549), increased fluorescence intensity was registered in these cells (Fig. 3c and d). Augmented cellular internalisation of other nanomaterials, like latex nanobeads or transferrin under K^+-depletion and chlorpromazine treatments was previously described in literature [24,26]. Taking together these results and ours, it seems that the efficiency of these inhibitory conditions (K^+-depletion and chlorpromazine) is correlated with the cellular type. Despite of these unexpected results, a slight reduction of cellular internalisation of MWCNT-FITC was observed with K^+-depleted A459 cells. We then investigated if the nanotubes were internalised by caveolae-mediated endocytosis, by inhibiting this mechanism using genistein and filipin III [23,25]. Under these conditions, up to 80% of MWCNT-FITC were still internalised by non-phagocytic cells while uptake in macrophages was not affected (Fig. 3e and f). It is important to note that some of the inhibitors (chlorpromazine, genistein or filipin III) did not affect the internalisation of uptake markers (transferrin and Bodipy) by macrophages. Indeed, we could not observe any difference in CNT uptake in RAW 264.7 as the inhibitory conditions did not efficiently block the clathrin or caveolae-mediated endocytosis even in the case of the uptake markers. Finally, macropinocytosis was inhibited by blocking the Na^+/K^+ exchange using amiloride and sequestering the membrane cholesterol with m-βCD [27,28]. In both cell lines, m-βCD treatment resulted in 20–30% inhibition of CNT uptake while amiloride was only efficient in blocking uptake in the non-phagocytic cell line, resulting in a slight but significant reduction in cellular internalisation of the CNTs (Fig. 3g and h).

Taking together all the flow cytometry results using both cell types, it was possible to notice that, while genistein, filipin III and amiloride slightly decreased the MWCNT-FITC cellular uptake in A549, these inhibitors did not affect internalisation in RAW 264.7 macrophages. Actually, neither genistein nor filipin III inhibitory conditions were effective in blocking uptake of the markers. On the contrary, a similar effect on cellular uptake was demonstrated at 4 °C, NaN_3 and m-βCD pre-treatment in both cell lines.

In order to confirm the presence of our CNTs inside the cells, we observed the MWCNT-FITC **3** uptake by RAW 264.7 macrophages in the presence of the different inhibitors (Table 1) using CLSM (Fig. 4). First of all, it was interesting to note that, in a general manner, the confocal results matched with the previous FACS analysis even for the fluorescently-labelled control molecules (transferrin, Bodipy and dextran; see ESI Figure S1) or the CNT treated cells. Fig. 4b and c displays how 4 °C and energy-depleted (NaN_3) conditions reduced the fluorescence signal in RAW 264.7 compared to the MWCNT-FITC **3** treatment alone, confirming the flow cytometry data. Furthermore, chlorpromazine, genistein, filipin III and amiloride (Fig. 4e–h) did not induce an appreciable modification of the CNT internalisation while the slight decrease in cellular uptake previously observed by flow cytometry with the m-βCD treatment was also observed by confocal microscopy (Fig. 4i). The only discrepancy between FACS and confocal microscopy results was related to K^+-depletion condition (Figs. 3c and 4d). In fact, it was possible to note that the fluorescence observed by CLSM was similar to the one of the MWCNT-FITC **3** alone while FACS analysis revealed a significant increase in the fluorescent signal. In our experimental conditions, it was possible to demonstrate that K^+-depletion is a condition that greatly alters the cell morphology. In fact, as it can be seen in the FSC/SSC data reported in the Supporting Information (ESI, Figure S2), cells incubated in the absence of potassium showed an augmented intracellular complexity, revealed by a shift in the SSC signal. We hypothesise that this change could determine a slight modification of the cellular autofluorescence intensity, sufficient to be revealed by flow cytometry but not enough to be seen by CLSM. On the other hand, it was not possible to detect any augmented fluorescence intensity by FACS when cells were incubated with K^+-depletion buffer alone (data not shown), excluding the possibility that autofluorescence derived from the morphological changes in cells pre-incubated in K^+-depleted conditions and exposed to MWCNTs could account for the increased fluorescence intensity we previously observed. Further experiment should be performed to better investigate this phenomenon, but this is beyond the purpose of the present study.

To further explore the intracellular localisation pattern of the uptaken CNTs at early time points, ultra-thin sections of A549 cells were prepared and examined by TEM after their incubation with ammonium-functionalised MWCNTs (MWCNT-NH_3^+ **2**) at 37 °C for periods from 15 to 120 min. In control cells maintained at 37 °C,

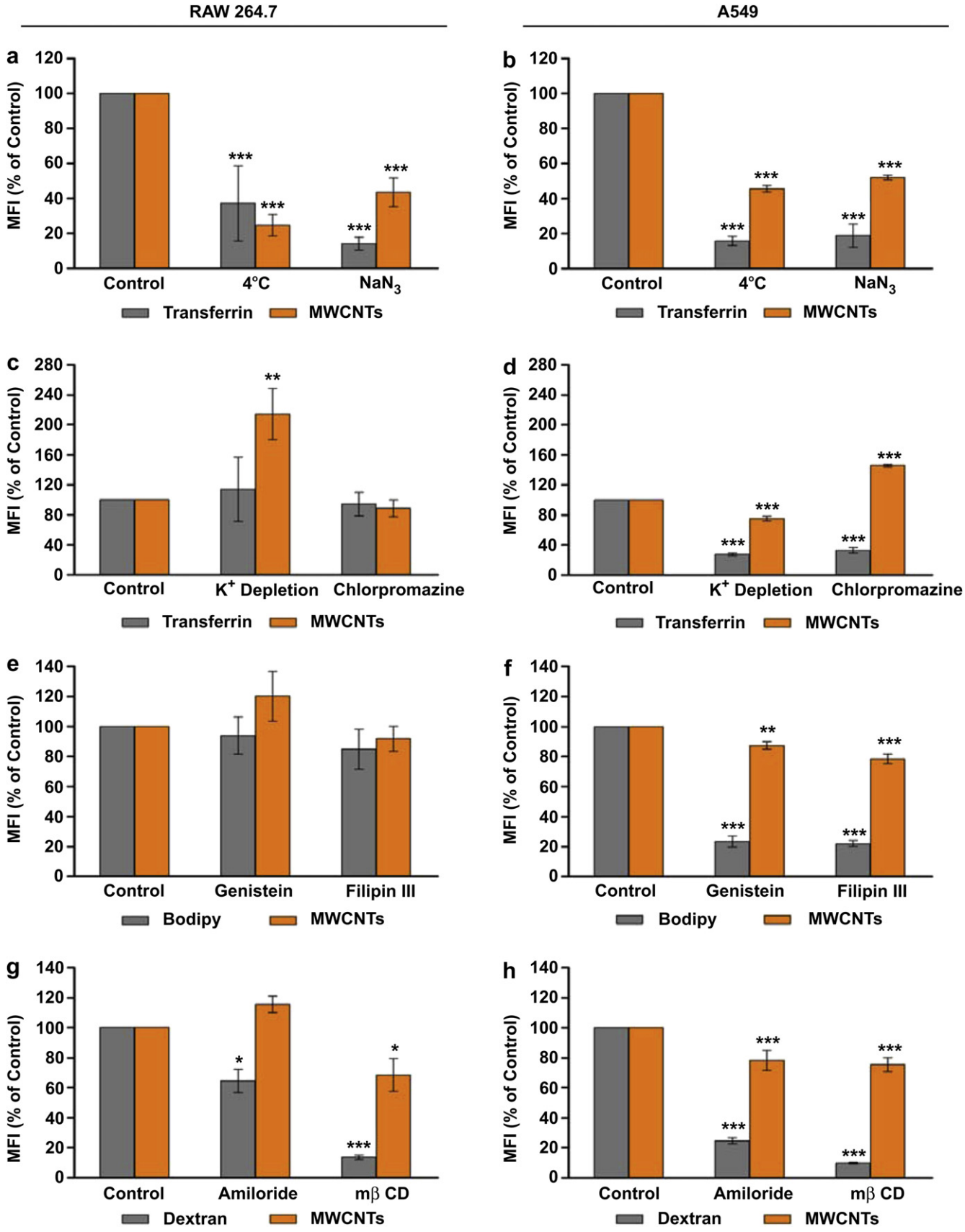

Fig. 3. Quantification of the extent of cellular uptake of MWCNT-FITC **3** and **4** in RAW 264.7 and A549, respectively, by flow cytometry. Conditions that inhibit different internalisation pathways were: energy-dependent internalisation (a and b), clathrin-mediated endocytosis (c and d), caveolae-mediated endocytosis (e and f) and macropinocytosis-dependent internalisation (g and h). Mean values ± SEM were obtained from at least three experiments run in triplicate. One-way ANOVA, followed by Dunnett's post test was carried out to determine the statistical significance of the data obtained with the different inhibitors compared to the control molecules or MWCNT-FITC alone ($^{*}p < 0.05$; $^{**}p < 0.01$; $^{***}p < 0.001$).

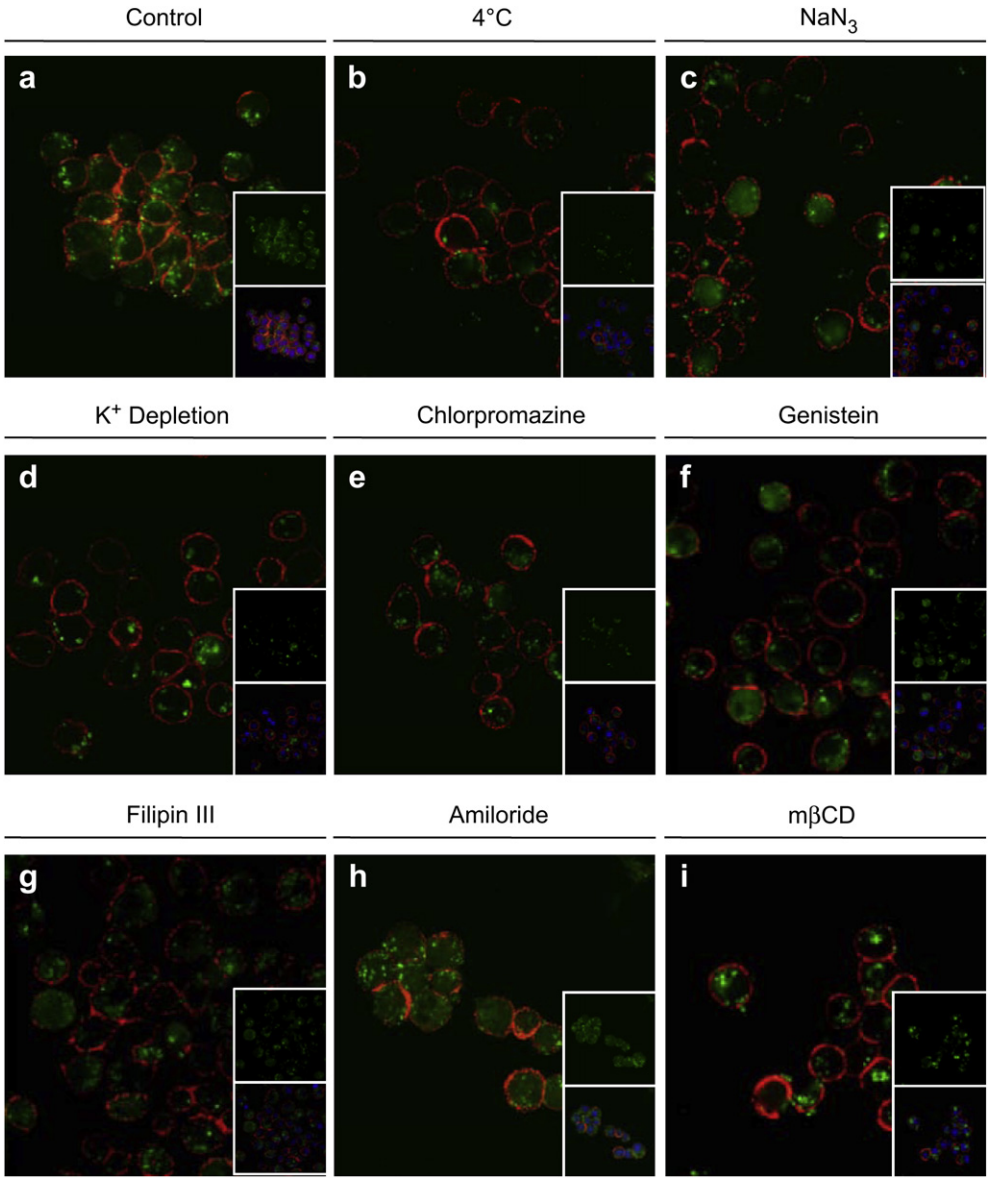

Fig. 4. Intracellular localisation of MWCNT-FITC **3** in RAW 264.7 cells using CLSM when cells were incubated with MWCNT-FITC **3** alone (a) or under conditions that inhibit the different internalisation pathways: energy-dependent internalisation (b and c), clathrin-mediated endocytosis (d and e), caveolae-mediated endocytosis (f and g) macropinocytosis-dependent internalisation (h and i). MWCNT-FITC localisation is indicated by green fluorescence while cellular membrane (CD11b labelling) is evidenced by red fluorescence and nuclei (DAPI staining) by blue fluorescence. The images represent one of at least three experiments with similar results.

intracellular organelles were identified (Fig. 5). We observed that a 15 min incubation period was sufficient to find individualised CNTs in the perinuclear area (Fig. 5a and b). After 30 min incubation, it was possible to find a higher number of individualised nanotubes in the cell cytoplasm (Fig. 5c and d). However, in the sections incubated for 60 min, the nanotubes were detected in clusters rather than individualised tubes without being surrounded by a distinct membrane (Fig. 5e and f). This could be due to the simple fact that 1 h of incubation allows the cells to gather more CNTs, which are then more apparent in the cytoplasm. Moreover, it is likely that the CNTs that cross the cellular membrane can do so thanks to their specific features (e.g. amphiphilicity) and that the same properties that account for the CNTs translocation towards the cellular membrane are also responsible for their translocation inside the cells.

After incubating the A549 cells for 2 h in the presence of MWCNT-NH_3^+ **2**, nanotubes were observed inside intracellular structures, confined within a membrane (Fig. 5g–i). It is interesting to note that although some nanotubes were occasionally found in this kind of compartments at the earlier time points, after 120 min of incubation the CNTs were mainly enclosed within membrane structures close to the cell nucleus.

These results are consistent with our observations by confocal microscopy that *f*-CNTs were taken up in a dose-dependent manner by mammalian cells and were localised in the perinuclear region in structures with a membrane enclosing the nanotubes [13,29] at the early time point incubations studied. However, we believe that the CNTs were enclosed inside multivesicular bodies after the internalisation process had occurred, because of the hydrophobic/hydrophilic character that will be determined by their carbon backbone and functional groups.

We then investigated whether or not incubation at 4 °C would affect the internalisation of MWCNT-NH_3^+ **2** by A459 after 30 and 60 min of incubation. TEM images reported in Fig. 6 show ultra-thin

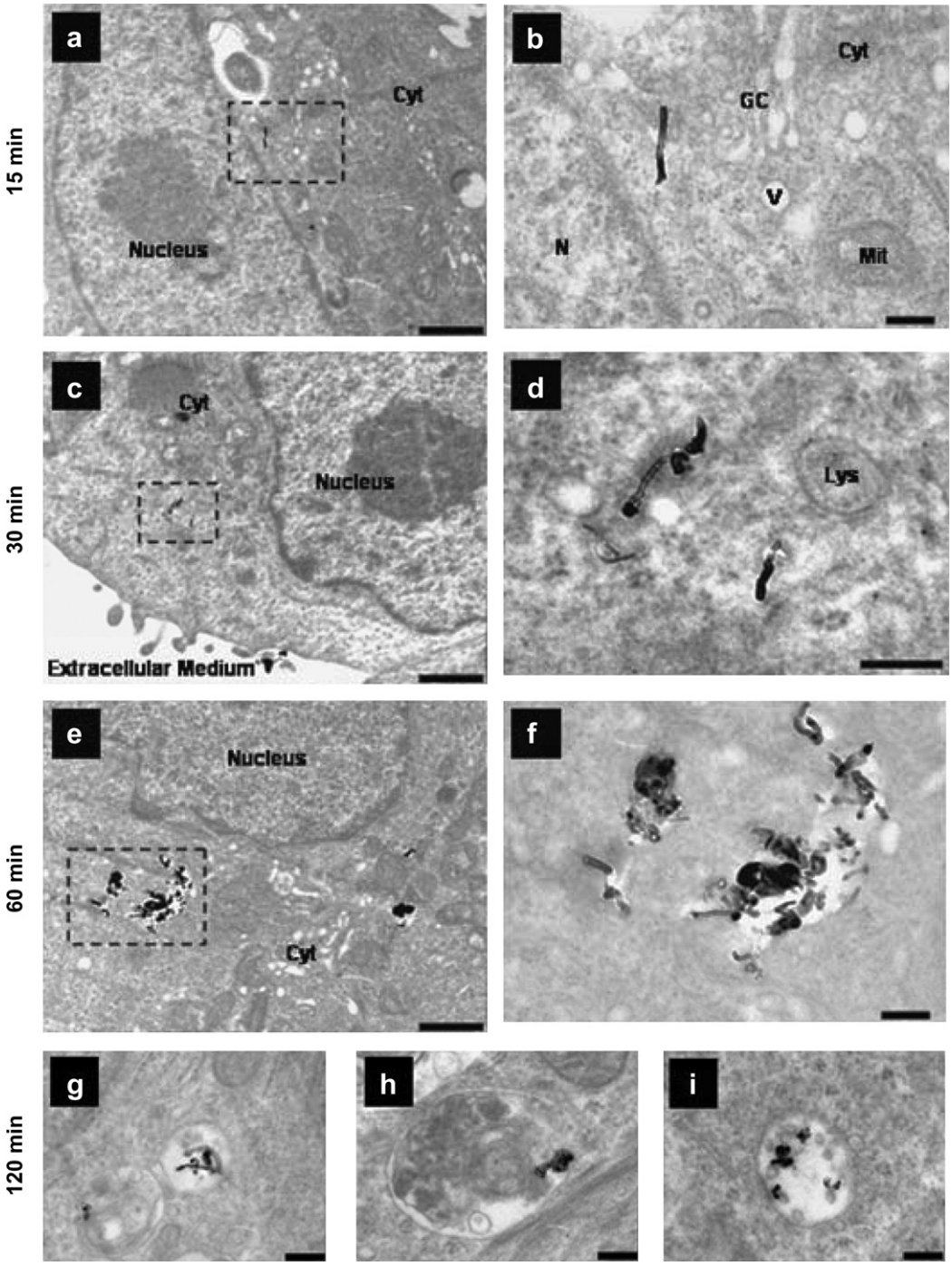

Fig. 5. Intracellular localisation of MWCNT-NH_3^+ **2** in A549 cells following 15 min incubation period at 37 °C (a and b), 30 min (c and d), 60 min (e and f) and 120 min (g–i). b, d and f are higher magnifications of the areas limited in a, c and e, respectively. Scale bars in a, c and e are of 1 μm, and 200 nm for remaining images. Cyt, cytoplasm; N, nucleus; GC, golgi complex; V, vesicle; Mit, mitochondria; Lys, lysosome.

sections of cells incubated with nanotubes during 60 min. In Fig. 6a two viewing areas were highlighted: one in the perinuclear region (white square) and another near the cell membrane (black square). These areas were magnified and it was possible to identify individualised nanotubes close to the cell nucleus (arrow in Fig. 6b) as previously observed after incubation at 37 °C, and in the second area several individualised nanotubes in the process of crossing the cell membrane (arrows in Fig. 6c) were also observed. It is noteworthy that at 4 °C, the CNTs were not entering the cells via any kind of membrane invagination process (e.g. clathrin-coated endocytosis) as that described earlier by Kam et al. [14] and others, confirming the passive diffusion of the CNTs across the plasma membrane. It is also important to mention that these nanostructures were not surrounded by any kind of membrane when incubated at 4 °C.

4. Discussion

One key advantage of chemically functionalised CNTs as drug delivery systems consists of their capacity to directly translocate

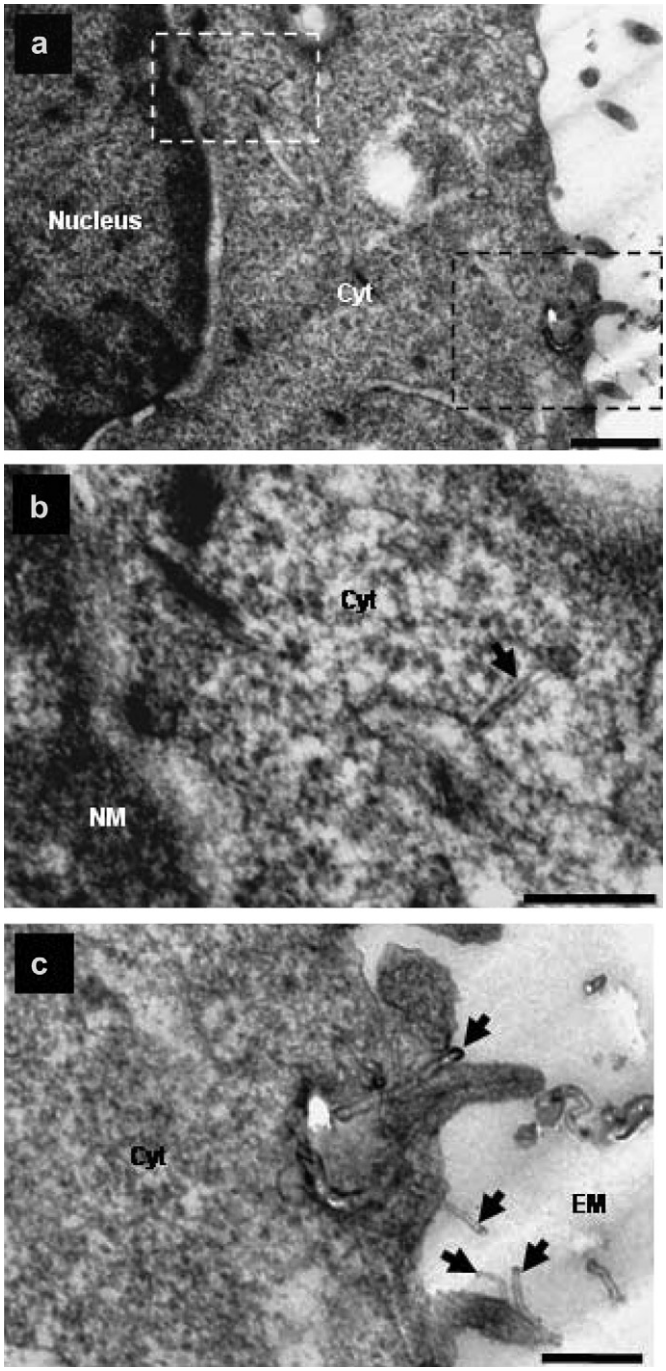

Fig. 6. Intracellular localisation of MWCNT-NH_3^+ **2** in A549 cells following 60 min incubation period at 4 °C. b is a higher magnification of the area limited in a with a white dashed line, and c is a higher magnification of the area limited in a with a black dashed line. Scale bars are 500 nm (a) and 200 nm (b and c). Cyt, cytoplasm; NM, nuclear membrane; EM, extracellular medium. Arrows are pointing to MWCNT-NH_3^+.

into the cytoplasm. Although *f*-CNTs have emerged as biocompatible systems with reduced toxic effects [1], the underlying mechanisms of their cellular uptake are still under investigation. The processes that regulate their cellular entry have been associated to two main pathways: i) energy-dependent internalisation; and ii) passive diffusion through the plasma membrane (similar to a "nanoneedle") [13–19]. In the present study, we report the *f*-MWCNTs uptake by phagocytic and non-phagocytic cells under inhibitory conditions of the different pathways responsible for exogenous molecule internalisation. The findings suggest that the internalisation of *f*-MWCNTs does not solely occur by one or the other previously reported mechanisms, but more probably by the combination of both. Our data herein showed that 30–50% of *f*-MWCNTs enter cells by a temperature-insensitive and energy-independent mechanism, further confirming that the hypothesis of a direct penetration across the cell membrane does occur (Fig. 6c) and at the same time that another fraction of the *f*-MWCNTs enter cells through a mix of energy-dependent mechanisms (endocytosis and macropinocytosis) (Fig. 3) [8,13,16,17,30,31].

Using phagocytic and non-phagocytic cell lines, we aimed to highlight possible differences in the mechanisms involved in the cellular uptake of *f*-MWCNTs. As a matter of fact, no discrepancy was observed in the internalisation of MWCNT-FITC by RAW 264.7 and A549 treated with the different uptake inhibitors (Fig. 3), although it seems that non-phagocytic cells were more sensitive to some inhibiting conditions even if higher concentrations of inhibitors were needed to achieve a significant reduction of cellular uptake (i.e. K^+-depletion, genistein, filipin III and amiloride). It is important to mention that under some inhibitory conditions using RAW 264.7 macrophages, it was not possible to achieve a significant reduction of the uptake markers which in turn makes it difficult to conclude if MWCNT cellular internalisation was not affected by some inhibitors (i.e. potassium depletion; chlorpromazine, genistein and filipin III). On the other hand, as cellular viability was the primary factor to keep in mind during these experiments, an increase of the inhibitor concentrations could not be envisaged. Nevertheless, when good inhibitory rates were obtained, the experimental data showed that in both cell lines, a large part of *f*-MWCNTs was internalised through a temperature-insensitive and energy-independent pathway, even in murine macrophages where we expected an almost exclusive contribution of endocytic pathways (Figs. 3 and 4). It is also important to note that we used MWCNTs functionalised with FITC or ammonium moieties which can be considered as small functional groups. In this way the nanotube surface was allowed to directly interact with the plasma membrane, which is consistent with the great fraction of tubes that penetrated cells under endocytosis inhibitory conditions. It was noteworthy that the inhibitory conditions were generally more efficient for the control molecules (transferrin, Bodipy and dextran) than for the MWCNT-FITC (Figs. 3 and 4, and Figure S1). This observation further corroborates the capacity of CNTs to translocate towards cellular membranes through non-specific, non-endocytic and non-phagocytic pathways.

In a recent work from our group, nanotube trafficking was reported by using 3D electron tomography imaging [8]. We observed *f*-CNTs penetrating into phagocytic and non-phagocytic cells by three alternative pathways: i) via membrane wrapping as individual tubes; ii) via direct membrane translocation of individual nanotubes; and iii) in bundles within vesicular compartments. These experimental observations were in agreement with another recent study where human monocyte derived macrophages were shown to internalise phospholipid-coated nanotube aggregates bigger than 400 nm via endocytosis while diffusion through the cellular membrane was also reported when the size of the bundles was lower than 400 nm [10]. Moreover, the capacity of *f*-CNTs to escape phagosomes after 14 days of incubation was also previously reported [8]. The mechanistic hypothesis that could be made is that CNTs, due to their hydrophobicity, have a preference for the lipid bilayer phase of cellular membranes. This hydrophobic affinity could be the reason for the CNT "nanoneedle" activity through the membranes, not only to enter cells, but also to evade endosomes or other intracellular

organelles once the CNTs are localised intracellularly. This hypothesis is consistent with the observation that the inhibitory conditions that mostly affect the plasma membrane functionality and structural arrangements (4 °C, NaN_3 and m-βCD) were also the conditions that lead to a significant decrease in the MWCNT-FITC internalised in both cell lines.

We also believe that the size and individualisation of the nanotubes play an important role in cellular uptake. *f*-MWCNTs with lengths around 100 nm should be able to fit in the clathrin and caveolae vesicles, while long tubes (>500 nm) and bundles or aggregates of tubes probably are uptaken by macropinocytosis. Nevertheless, well-individualised *f*-MWCNTs with lengths around 300–400 nm were shown to be able to cross cell membranes. Such alternative internalisation mechanisms can have a direct impact on the delivery of drugs, proteins and nucleic acids, since the nanotubes seem to be able to rapidly enter the cells and freely traffic in the cytoplasm (not enclosed by membrane structures) within 1 h after internalisation (Fig. 5). In particular, if we consider the potential risk of inactivation of therapeutics by a number of acid hydrolases from the endo-lysosomal compartment, nanotube-based drug delivery systems that could escape the endocytotic/phagocytic pathways would be of great interest.

On the other hand, the fate of CNTs after cellular internalisation could be also influenced by their ability to easily cross the cellular membranes. The fact that CNTs can be found free in the cytoplasm (Figs. 5a–f and 6a and b) after a short incubation time supports their ability to escape from the phagosomes [8], thus preventing their elimination via endo-lysosomal/phago-lysosomal vesicles. In addition, we observed that free CNTs can be wrapped into endosome-like structures after a longer incubation time (2 h, Fig. 5g–i). In this case, the formation of endo-lysosomal vesicle would be possible, then allowing the contact of the internalised CNTs with the lysosomal enzymes, leading to their possible enzymatic degradation [32–34]. Preliminary observations from ongoing studies in our laboratories attempting to characterise the nature of the intracellular compartments in which *f*-CNTs reside at different time points, indicate that lysosomes play an important role in these processes. Also, further studies are needed to investigate the trafficking and fate of the internalised CNTs after longer incubation times than those considered in the present paper. These experiments could possibly help understand how *f*-CNTs are processed by cells, and more importantly if there are some particular characteristics that promote the elimination and/or biodegradation of the internalised CNTs, which is also of great interest towards their biomedical utilisation.

5. Conclusions

The current study illustrated the significant contribution that plasma membrane translocation has in the cellular uptake of CNTs. This data further confirms that multiple internalisation pathways may simultaneously operate and determine CNT cellular uptake and trafficking. Furthermore, the balance between the possible mechanisms in operation will be strongly dependent on the type of CNT functionalisation (i.e. small organic groups or molecules against macromolecules or biopolymers like lipids, proteins or DNA), the physicochemical nature of the CNT dispersions (i.e. individualisation against small or large bundles) and the type of cells (i.e. non-phagocytic against phagocytic cells). In general, we would like to conclude that there can be no single, unique mechanism responsible for CNT cellular uptake, and that chemical functionalisation could represent a way to tailor the fate of CNTs by tilting the balance towards specific mechanisms of internalisation, cellular processing and elimination/degradation depending on the desired application.

Acknowledgements

This work was supported by The School of Pharmacy, University of London, by CNRS and the Agence Nationale de la Recherche (grant ANR-05-JCJC-0031-01), the Italian Ministry of Education MIUR (cofin Prot. 20085M27SS and FIRB prot. RBAP11ETKA), and by the European Union through the ERC Advanced Grant Carbonanobridge (contract ERC ADG 2008 – Grant Agreement 227135), and Regione Friuli-Venezia Giulia. L.L. acknowledges support by the Portuguese Foundation for Science and Technology (FCT/MCTES) for the award of a PhD fellowship (Ref. SFRH/BD/21845/2005). J.R. is grateful to the European Union FP7 ANTICARB (HEALTH-2007-201587) program. The authors wish to thank S. Lacotte for the preliminary experiments on macrophage CNT uptake. A.B. wishes to acknowledge the CNRS financial support from PICS (Project for International Scientific Cooperation).

Appendix. Supplementary material

Supplementary data associated with this article can be found, in the online version, at doi:10.1016/j.biomaterials.2012.01.024.

References

[1] Kostarelos K, Bianco A, Prato M. Promises, facts and challenges for carbon nanotubes in imaging and therapeutics. Nat Nanotechnol 2009;4:627–33.
[2] Bianco A. Carbon nanotubes for the delivery of therapeutic molecules. Expert Opin Drug Deliv 2004;1:57–65.
[3] Hong SY, Tobias G, Al-Jamal KT, Ballesteros B, Ali-Boucetta H, Lozano-Perez S, et al. Filled and glycosylated carbon nanotubes for in vivo radioemitter localization and imaging. Nat Mater 2010;9:485–90.
[4] Lacerda L, Raffa S, Prato M, Bianco A, Kostarelos K. Cell-penetrating carbon nanotubes in the delivery of therapeutics. Nano Today 2007;2:38–43.
[5] Liu Z, Tabakman S, Welsher K, Dai H. Carbon nanotubes in biology and medicine: in vitro and in vivo detection, imaging and drug delivery. Nano Res 2009;2:85–120.
[6] Raffa V, Ciofani G, Vittorio O, Riggio C, Cuschieri A. Physicochemical properties affecting cellular uptake of carbon nanotubes. Nanomedicine (Lond) 2010;5:89–97.
[7] Lamm MH, Ke PC. Cell trafficking of carbon nanotubes based on fluorescence detection. Methods Mol Biol 2010;625:135–51.
[8] Al-Jamal KT, Nerl H, Müller KH, Ali-Boucetta H, Li S, Haynes PD, et al. Cellular uptake mechanisms of functionalised multi-walled carbon nanotubes by 3D electron tomography imaging. Nanoscale 2011;3:2627–35.
[9] Kang B, Chang S, Dai Y, Yu D, Chen D. Cell response to carbon nanotubes: size-dependent intracellular uptake mechanism and subcellular fate. Small 2010;6:2362–6.
[10] Antonelli A, Serafini S, Menotta M, Sfara C, Pierigé F, Giorgi L, et al. Improved cellular uptake of functionalized single-walled carbon nanotubes. Nanotechnology 2010;21:425101.
[11] Mu Q, Broughton DL, Yan B. Endosomal leakage and nuclear translocation of multiwalled carbon nanotubes: developing a model for cell uptake. Nano Lett 2009;9:4370–5.
[12] Zhang X, Meng L, Wang X, Lu Q. Preparation and cellular uptake of pH-dependent fluorescent single-wall carbon nanotubes. Chemistry 2010;16:556–61.
[13] Kostarelos K, Lacerda L, Pastorin G, Wu W, Wieckowski S, Luangsivilay J, et al. Cellular uptake of functionalized carbon nanotubes is independent of functional group and cell type. Nat Nanotechnol 2007;2:108–13.
[14] Kam NW, Liu Z, Dai H. Carbon nanotubes as intracellular transporters for proteins and DNA: an investigation of the uptake mechanism and pathway. Angew Chem Int Ed Engl 2006;45:577–81.
[15] Pantarotto D, Briand JP, Prato M, Bianco A. Translocation of bioactive peptides across cell membranes by carbon nanotubes. Chem Commun (Camb); 2004:16–7.
[16] Pantarotto D, Singh R, McCarthy D, Erhardt M, Briand JP, Prato M, et al. Functionalized carbon nanotubes for plasmid DNA gene delivery. Angew Chem Int Ed Engl 2004;43:5242–6.
[17] Lopez CF, Nielsen SO, Moore PB, Klein ML. Understanding nature's design for a nanosyringe. Proc Natl Acad Sci U S A 2004;101:4431–4.
[18] Shi Kam NW, Jessop TC, Wender PA, Dai H. Nanotube molecular transporters: internalisation of carbon nanotube-protein conjugates into mammalian cells. J Am Chem Soc 2004;126:6850–1.
[19] Kam NW, Dai H. Carbon nanotubes as intracellular protein transporters: generality and biological functionality. J Am Chem Soc 2005;127:6021–6.
[20] Georgakilas V, Kordatos K, Prato M, Guldi DM, Holzinger M, Hirsch A. Organic functionalization of carbon nanotubes. J Am Chem Soc 2002;124:760–1.

[21] Serag MF, Kaji N, Gaillard C, Okamoto Y, Terasaka K, Jabasini M, et al. Trafficking and subcellular localization of multiwalled carbon nanotubes in plant cells. ACS Nano 2011;5:493–9.
[22] Gaillard C, Cellot G, Li S, Toma FM, Dumortier H, Spalluto G, et al. Carbon nanotubes carrying cell adhesion peptides do not interfere with neuronal functionality. Adv Mater 2009;21:2903–8.
[23] Marks DL, Singh RD, Choudhury A, Wheatley CL, Pagano RE. Use of fluorescent sphingolipid analogs to study lipid transport along the endocytic pathway. Methods 2005;36:186–95.
[24] Vercauteren D, Vandenbroucke RE, Jones AT, Rejman J, Demeester J, De Smedt SC, et al. The use of inhibitors to study endocytic pathways of gene carriers: optimization and pitfalls. Mol Ther 2010;18:561–9.
[25] Rejman J, Bragonzi A, Conese M. Role of clathrin- and caveolae-mediated endocytosis in gene transfer mediated by lipo- and polyplexes. Mol Ther 2005;12:468–74.
[26] Rejman J, Oberle V, Zuhorn IS, Hoekstra D. Size-dependent internalization of particles via the pathways of clathrin- and caveolae-mediated endocytosis. Biochem J 2004;377:159–69.
[27] Mano M, Teodósio C, Paiva A, Simões S, Pedroso de Lima MC. On the mechanisms of the internalization of S4(13)-PV cell-penetrating peptide. Biochem J 2005;390:603–12.
[28] von Delwig A, Hilkens CM, Altmann DM, Holmdahl R, Isaacs JD, Harding CV, et al. Inhibition of macropinocytosis blocks antigen presentation of type II collagen in vitro and in vivo in HLA-DR1 transgenic mice. Arthritis Res Ther 2006;8:R93.
[29] Lacerda L, Pastorin G, Gathercole D, Prato M, Bianco A, Kostarelos K. Intracellular trafficking of carbon nanotubes by confocal laser scanning microscopy. Adv Mater 2007;19:1480–4.
[30] Rojas-Chapana J, Troszczynska J, Firkowska I, Morsczeck C, Giersig M. Multiwalled carbon nanotubes for plasmid delivery into *Escherichia coli* cells. Lab Chip 2005;5:536–9.
[31] Kateb B, Van Handel M, Zhang L, Bronikowski MJ, Manohara H, Badie B. Internalization of MWCNTs by microglia: possible application in immunotherapy of brain tumors. Neuroimage 2007;37(Suppl. 1):S9–17.
[32] Russier J, Ménard-Moyon C, Venturelli E, Gravel E, Marcolongo G, Meneghetti M, et al. Oxidative biodegradation of single- and multi-walled carbon nanotubes. Nanoscale 2011;3:893–6.
[33] Zhao Y, Allen BL, Star A. Enzymatic degradation of multiwalled carbon nanotubes. J Phys Chem A 2011;115:9536–44.
[34] Kagan VE, Konduru NV, Feng W, Allen BL, Conroy J, Volkov Y, et al. Carbon nanotubes degraded by neutrophil myeloperoxidase induce less pulmonary inflammation. Nat Nanotechnol 2010;5:354–9.